Estimation of the direction of the coupling by conditional probabilities of recurrence

M. Carmen Romano,[1,*] Marco Thiel,[1] Jürgen Kurths,[2] and Celso Grebogi[1]
[1]*College of Physical Sciences, King's College, University of Aberdeen, Aberdeen AB24 3UE, United Kingdom*
[2]*Nonlinear Dynamics, Institute of Physics, University of Potsdam, 14469 Potsdam, Germany*
(Received 28 February 2007; revised manuscript received 14 May 2007; published 21 September 2007)

We introduce a method to detect and quantify the asymmetry of the coupling between two interacting systems based on their recurrence properties. This method can detect the direction of the coupling in weakly as well as strongly coupled systems. It even allows detecting the asymmetry of the coupling in the more challenging case of structurally different systems and it is very robust against noise. We also address the problem of detecting the asymmetry of the coupling in passive experiments, i.e., when the strength of the coupling cannot be systematically changed, which is of great relevance for the analysis of experimental time series.

DOI: 10.1103/PhysRevE.76.036211 PACS number(s): 05.45.Xt, 82.40.Bj, 05.45.Ac

I. INTRODUCTION

The interplay among different complex dynamical systems is a central issue in nonlinear dynamics as well as in nonlinear time series analysis. Under certain assumptions different types of synchronization can occur between the interacting systems. This topic has been intensively studied in the last years and has been observed in various fields, such as physics, engineering, and biology [1,2]. In such systems it is important not only to analyze the synchronization but also to identify causal (drive-response) or mutual relationships. There are three major approaches to address this problem: state-space based methods [3–5], information theory based methods [6,7], and methods based on the interrelations between the phases of the systems under consideration [8].

In the state-space based approach, the state vectors are usually reconstructed by means of delay embedding [9]. The direction of the coupling is then assessed by considering the correspondence between neighbors in the phase spaces of the driver and response. If there exists a functional relationship between the driver X and the response system Y, i.e., $\vec{y}(t) = \Psi(\vec{x}(t))$, they are said to be generalized synchronized [10,11]. If Ψ exists and is smooth, it follows that close states of the driver will be mapped to close states of the response. However, if Ψ is bijective, also close states of the response will be mapped to close states of the driver. Therefore, if X and Y are generalized synchronized it is, in general, impossible to assess the direction of the coupling reliably and the state-space based methods are only applicable in the nonsynchronized regime [12].

There are several methods based on information theory to determine the direction of the coupling [6,7]. They are usually applied to systems which are strongly coupled. In order to also treat weakly coupled systems, the phases of the signals are determined beforehand, and then information theory based indices are applied to the phases [13].

In Ref. [8], a technique based on the fitting of the functional relationship between the phases of the two interacting systems has been proposed to detect and quantify the asymmetry in the coupling.

Smirnov and Andrzejak have systematically compared the phase dynamics to the state-space approach in the case of weak directional coupling [12]. They concluded that neither one of the approaches is generally superior and that both approaches have difficulties in assessing the direction of the coupling in systems which are structurally different.

In this paper, we introduce a method to uncover directional coupling. This approach is based on the recurrence properties of both interacting systems. The concept of recurrence has been used to detect relationships between interacting systems in [14], where the so-called synchronization likelihood has been introduced. This method allows for a multivariate analysis of generalized synchronization. Moreover, in [15] the concept of recurrence has been used to quantify a weaker form of synchronization, namely phase synchronization. Here, we extend these measures in order to detect the direction of the coupling. The proposed method is rather straightforward to compute, in contrast to the more complicated information theory approaches. Furthermore, it has the advantage that it is applicable to both weak and strong directional coupling, as well as to structurally different systems.

The outline of this paper is as follows: in Sec. II we introduce measures for the analysis of the directional coupling based on recurrences. In Sec. III we demonstrate the proposed measures in some numerical examples and discuss the choice of the parameters of the method in Sec. IV. In Sec. V we discuss the dependence of these measures on observational noise. We consider in Sec. VI the problem of passive experiments, where the coupling strength between the two interacting systems cannot be varied systematically. In Sec. VII we compare the proposed method with other existing techniques and, finally, we give some conclusions.

II. DETECTION OF THE COUPLING DIRECTION BY RECURRENCES

Recurrence is a fundamental property of dynamical systems. The concept of recurrence was introduced by Poincaré [16], where he showed that the trajectory of a dynamical system with a measure preserving flow recurs infinitely many times to some neighborhood of a former visited state on an invariant set in phase space. There are many different

*Corresponding author; m.romano@abdn.ac.uk

techniques in nonlinear dynamics which exploit the concept of recurrence [17–19]. We concentrate on the method of recurrence plots (RPs), introduced by Eckmann *et al.* to visualize the behavior of dynamical systems in the phase space [20]. They are defined by means of the recurrence matrix

$$R_{i,j}^{X} = \Theta(\varepsilon - \|\vec{x}_i - \vec{x}_j\|), \quad i,j = 1, \ldots, N, \tag{1}$$

where $\vec{x}_i$ denotes the state of the system X at time $i\Delta t$ with Δt being the sampling rate, ε is a predefined threshold, $\Theta(\cdot)$ is the Heaviside function, and N is the length of the trajectory considered. The RP is obtained plotting a black dot at the coordinates (i,j) if $R_{i,j}=1$. By looking at the patterns of the RP, one obtains at the outset a visual impression about the dynamics of the system under consideration. In order to go beyond the visual impression, several measures have been proposed to quantify the patterns in the RP. They have found numerous applications in very different kinds of systems [21,22]. Moreover, somehow more formal relationships between the patterns obtained in RPs and main dynamical invariants, such as K_2 and D_2, have been found [23]. It has also been shown that the RP contains all necessary information to reconstruct the underlying trajectory, at least topologically [24].

The method of RPs has been extended to joint recurrence plots (JRPs) to analyze the interplay of two or more dynamical systems [14,25]. The JRP of X and Y is defined as follows:

$$J_{Ri,j}^{X,Y} = \Theta(\varepsilon_X - \|\vec{x}_i - \vec{x}_j\|)\Theta(\varepsilon_Y - \|\vec{y}_i - \vec{y}_j\|), \tag{2}$$

i.e., a joint recurrence occurs if the system X recurs in its own phase space and simultaneously, the system Y recurs also in its own phase space. Based on JRPs it is possible to analyze different kinds of synchronization of coupled complex systems [14,15,26]. In order to illustrate this, we consider two rather different chaotic oscillators, namely the Rössler system

$$\begin{aligned} \dot{x}_1 &= 2 + x_1(x_2 - 4), \\ \dot{x}_2 &= -x_1 - x_3, \\ \dot{x}_3 &= x_2 + 0.45x_3, \end{aligned} \tag{3}$$

which drives the Lorenz system

$$\begin{aligned} \dot{y}_1 &= -10(y_1 - y_2), \\ \dot{y}_2 &= 28u - y_2 - uy_3, \\ \dot{y}_3 &= uy_2 - 8/3y_3, \end{aligned} \tag{4}$$

by means of the variable $u=x_1+x_2+x_3$. In [11] it has been shown that the driven Lorenz system is asymptotically stable and that both systems are in generalized synchronization. Hence, two close neighbors in the phase space of the driver system correspond to two close neighbors in the phase space of the driven system [10]. This relationship is reflected very clearly in the RPs of both systems. In Figs. 1(a) and 1(c) we plot the trajectories in phase space of the Rössler [Eq. (3)] and of the Lorenz system [Eq. (4)], respectively. To calculate

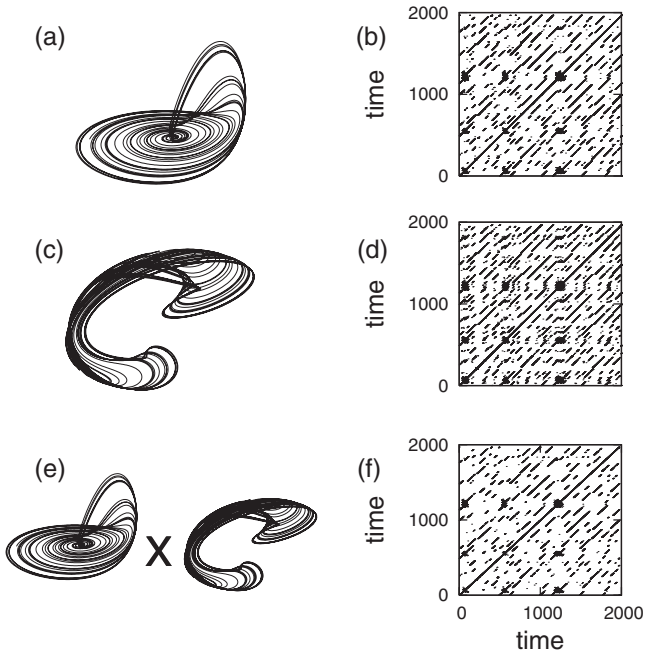

FIG. 1. (a) Rössler driving system, (b) the RP of the Rössler system $(m=3,\tau=5)$, (c) the driven Lorenz system, (d) the RP of the Lorenz system $(m=7,\tau=5)$, (e) representation of the "joint" system, and (f) the joint recurrence plot of both systems. The threshold for the computation of the RPs has been chosen so that the recurrence rate (number of recurrence points divided by N^2) is equal for both systems. In this case the recurrence rate was 0.005. The equations were integrated using fourth order Runge-Kutta and the sampling time was 0.2.

their corresponding RPs, we have used the third component of each system and reconstructed the respective trajectories in phase space using delay embedding [9] with embedding dimension $m=7$ and time delay $\tau=5$ (the time step between two consecutive points being 0.2), since dealing with experimental time series, usually only one observable of the system is available. Even though the shapes of both attractors in the phase space look rather different [Figs. 1(a) and 1(c)], both RPs are very similar [Figs. 1(b) and 1(d)]. Therefore, the joint recurrence plot [Fig. 1(f)] resembles the same recurrence patterns as the RPs of the single systems.

This property of joint recurrence plots has been treated in detail in [15], where it has been used for the detection of generalized synchronization, also in more difficult cases where other methods, such as the mutual false nearest neighbors, are not appropriate any longer. In [14] the authors have introduced the synchronization likelihood, which is a multivariate measure for generalized synchronization. This measure is based on a very similar concept to the joint recurrence matrix of Eq. (2). However, the thresholds ε_X and ε_Y are not fixed for the whole trajectories, but are dependent on time.

However, only considering the concept of joint recurrence is not sufficient to identify which system is the driver and which one is the response. In order to accomplish that, it is necessary to consider conditional probabilities of recurrence. Therefore, we propose the mean conditional probabilities of recurrence (MCR) between two systems X and Y, which are defined as follows:

$$M_{CR}(Y|X) = \frac{1}{N}\sum_{i=1}^{N} p(\vec{y}_i|\vec{x}_i) = \frac{1}{N}\sum_{i=1}^{N} \frac{\sum_{j=1}^{N} J_{Ri,j}^{X,Y}}{\sum_{j=1}^{N} R_{i,j}^{X}} \tag{5}$$

and

$$M_{CR}(X|Y) = \frac{1}{N}\sum_{i=1}^{N} p(\vec{x}_i|\vec{y}_i) = \frac{1}{N}\sum_{i=1}^{N} \frac{\sum_{j=1}^{N} J_{Ri,j}^{X,Y}}{\sum_{j=1}^{N} R_{i,j}^{Y}}, \tag{6}$$

where $p(\vec{y}_i|\vec{x}_i)$ is an estimate of the probability that the trajectory of Y recurs to the neighborhood of $\vec{y}_i$ under the condition that the trajectory of X recurs to the neighborhood of $\vec{x}_i$ [$p(\vec{x}_i|\vec{y}_i)$ is defined analogously]. One can consider these measures as an extension of the methods presented in [14,15].

The criterion that we use for detecting the asymmetry of the coupling is the following:

$$\text{if } X \text{ drives } Y, \quad M_{CR}(Y|X) < M_{CR}(X|Y), \tag{7a}$$

$$\text{if } Y \text{ drives } X, \quad M_{CR}(X|Y) < M_{CR}(Y|X). \tag{7b}$$

If the coupling is symmetric, then $M_{CR}(X|Y)=M_{CR}(Y|X)$.

This criterion might appear counterintuitive at first, because if X is the driver, one could think that the probability of recurrence of a state $\vec{y}_i$ given that the state $\vec{x}_i$ recurs is larger than vice versa, since X is independent of Y.

A heuristic argumentation for this criterion is the following: if X drives Y, the dimension of Y, in general, will be larger than the dimension of X, because the evolution of Y is determined by both the states of X and Y. Moreover, the higher the complexity of Y, the smaller is the probability of recurrence of $\vec{y}_i \forall i$. Hence, increasing the coupling strength from X to Y, the probability $p(\vec{y}_i)$ that the trajectory of Y recurs to the neighborhood of $\vec{y}_i$ will decrease. In contrast, the complexity of X remains constant with increasing coupling strength, because the evolution of X depends only on the states of X. Hence, the probability $p(\vec{x}_i)$ that the trajectory of X recurs to the neighborhood of $\vec{x}_i$ does not change with the coupling strength. We choose the thresholds ε_X and ε_Y in such a way that if the coupling strength is equal to zero, $\langle p(\vec{x}_i)\rangle = \langle p(\vec{y}_i)\rangle$. Therefore, if the coupling strength from X to Y is larger than zero, in general $p(\vec{y}_i) < p(\vec{x}_i)$. That implies $p(\vec{x}_i,\vec{y}_i)/p(\vec{x}_i) < p(\vec{x}_i,\vec{y}_i)/p(\vec{y}_i)$ and hence, $M_{CR}(Y|X) < M_{CR}(X|Y)$.

III. NUMERICAL EXAMPLES

In this section we illustrate the performance of the proposed measures for the direction of the coupling by three kinds of examples: strongly coupled systems (close to the onset of complete synchronization), weakly coupled systems (close to the onset of phase synchronization), and structurally different systems. The number of data points of the trajectories used in each case, if not stated otherwise, is equal to 10 000 throughout the paper.

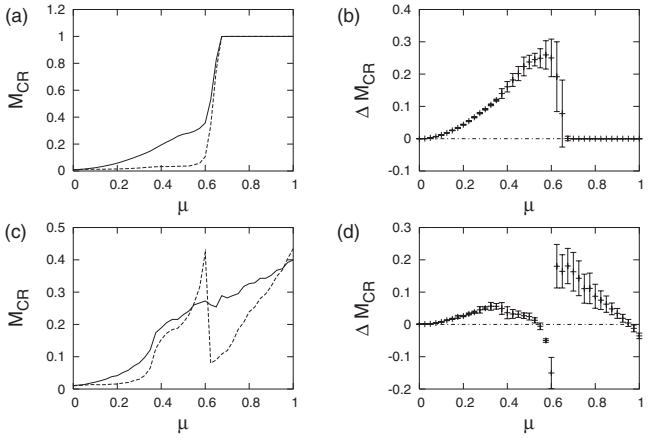

FIG. 2. Mean conditional probabilities of recurrence $M_{CR}(X|Y)$ (solid) and $M_{CR}(Y|X)$ (dashed) for two unidirectionally coupled identical (a) and nonidentical (c) Hénon maps. The system X is in both cases the driver, and hence, $M_{CR}(X|Y) > M_{CR}(Y|X)$. For each value of the coupling strength μ, the mean value over 100 trajectories for uniformly distributed initial conditions has been computed. In (b) and (d) we have plotted the mean value of the difference $\Delta M_{CR}=M_{CR}(X|Y)-M_{CR}(Y|X)$ over 100 trajectories and the corresponding standard deviation for the identical and nonidentical Hénon systems, respectively. The zero line is also plotted for orientation (dotted-dashed-line).

A. Strongly coupled systems

We consider two unidirectionally coupled Hénon maps, given by the following equations

$$x_1(i+1) = 1.4 - x_1(i)^2 + b_1 x_2(i),$$

$$x_2(i+1) = x_1(i), \tag{8}$$

for the driving system X, and

$$y_1(i+1) = 1.4 - [\mu x_1(i) y_1(i) + (1-\mu) y_1^2(i)] + b_2 y_2(i),$$

$$y_2(i+1) = y_1(i), \tag{9}$$

for the response system Y [5], where μ is the coupling strength. We analyze both the case of identical systems ($b_1=b_2=0.3$) and nonidentical systems ($b_1=0.1$, $b_2=0.3$). To mimic this problem for data analysis, we assume that we have observed the two scalar time series $\{x_1(i)\}_{i=1}^{N}$ and $\{y_1(i)\}_{i=1}^{N}$. Hence, we have to reconstruct the trajectories of X and Y in phase space [9]; this will be done by delay embedding. We choose embedding dimension $m=3$ and time delay $\tau=1$, but we note that the results are qualitatively the same with other reasonable choices. The values of the thresholds ε_X and ε_Y have been chosen such that for no coupling both mean probabilities of recurrences $\langle p(\vec{x}(i))\rangle$ and $\langle p(\vec{y}(i))\rangle$ are equal to 0.01. We use 10 000 data points and compute the indices $M_{CR}(X|Y)$ and $M_{CR}(Y|X)$ in dependence on the coupling strength μ. The results are shown in Fig. 2.

For two identical Hénon maps [Fig. 2(a)], the onset to identical synchronization occurs at approximately $\mu=0.65$, as reported in [5,7]. As expected from this, we yield for $\mu>0.65$, $M_{CR}(X|Y)=M_{CR}(X|Y)$. Before the onset of synchronization, we obtain $M_{CR}(X|Y)>M_{CR}(Y|X)$, indicating correctly the direction of the coupling.

On the other hand, for the nonidentical Hénon maps, the onset to generalized synchronization occurs at approximately $\mu=0.4$ [5]. Note that in general the detection of the directionality is only possible before the onset of synchronization. In the case of identical synchronization, the series $\{x_i\}$ and $\{y_i\}$ are identical and hence there is no possibility of establishing the causal relationship between X and Y just from the data. This argument can also be extended to the case of generalized synchronization, where the systems are related by a one-to-one function [4]. Therefore, in the case of the two nonidentical Hénon maps the directionality parameters are reliable for $0<\mu<0.4$. The sharp drop of $M_{CR}(Y|X)$ [dashed curve in Fig. 2(c)] at approximately $\mu=0.6$ is due to the nonmonotonic dependence of the maximum Lyapunov exponent of the response system on the coupling strength [5].

B. Weakly coupled systems

Now we study two nonidentical unidirectionally coupled Lorenz systems, given by the equations

$$\dot{x}_1 = 10(x_1 - x_2),$$

$$\dot{x}_2 = 40x_1 - x_2 - x_1x_3,$$

$$\dot{x}_3 = x_1x_2 - 8/3x_3, \tag{10}$$

for the driver system X and

$$\dot{y}_1 = 10(y_2 - y_1) + \mu(x_1 - y_1),$$

$$\dot{y}_2 = 35y_1 - y_2 - y_1y_2,$$

$$\dot{y}_3 = y_1y_2 - 8/3y_3, \tag{11}$$

for the response system Y. The equations have been integrated by a fourth-order Runge-Kutta algorithm and the time step between two consecutive points is equal to 0.03. We use 10 000 data points and assume that only the scalar variables x_3 and y_3 have been observed. The embedding parameters used for the reconstruction are $m=10$ and $\tau=12$. As in the former case, the results do not depend on the details of this choice. We have not used the optimal embedding parameters which can be estimated by, e.g., the methods of false nearest neighbors and the autocorrelation function, in order to show that the results are robust with respect to different embedding parameters [12]. We compute the directionality parameters MCR in dependence on the coupling strength μ between 0 and 10, which is before the onset of phase synchronization [12]. The results are shown in Figs. 3(a) and 3(b). We clearly see that $M_{CR}(X|Y)>M_{CR}(Y|X)$ for all computed values of the coupling strength μ, i.e., the recurrence based indices detect the direction of the coupling correctly. The values of

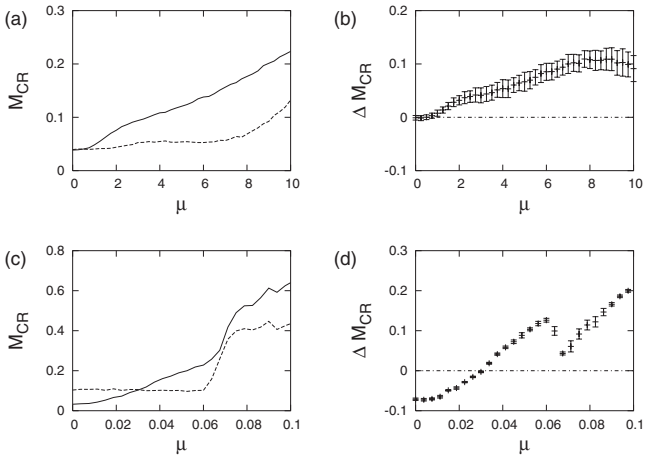

FIG. 3. Mean conditional probabilities of recurrence $M_{CR}(X|Y)$ (solid) and $M_{CR}(Y|X)$ (dashed) for (a) two weakly unidirectionally coupled nonidentical Lorenz systems. For each value of the coupling strength μ, the mean value over 100 trajectories for uniformly distributed initial conditions has been computed. The system X is the driver, and hence, $M_{CR}(X|Y)>M_{CR}(Y|X)$. (c) Two weakly bidirectionally coupled stochastic Van der Pol oscillators. The coupling strength from X to Y is fixed and equal to 0.03. In (b) and (d) we have plotted the mean value of $\Delta M_{CR}=M_{CR}(X|Y)-M_{CR}(Y|X)$ and the corresponding standard deviation over 100 trajectories for each system, respectively. The zero line is also plotted for orientation (dotted-dashed-line).

the thresholds ε_X and ε_Y have been chosen such that for no coupling both mean probabilities of recurrences $\langle p(\vec{x}(i))\rangle$ and $\langle p(\vec{y}(i))\rangle$ are equal to 0.01. However, note that for $\mu=0$, the values of $M_{CR}(X|Y)$ and $M_{CR}(Y|X)$ are larger and not equal to 0.01, as one would expect. This is because the estimated joint probability of recurrence is larger than $(0.01)^2$, due to the limited number of data used for the computation. Nevertheless, the expected qualitative behavior, i.e., $M_{CR}(X|Y)>M_{CR}(Y|X)$ still holds, which is the important fact for our analysis.

The next example that we consider is a bidirectionally coupled system, namely, two stochastic Van der Pol oscillators with slightly different mean frequencies ω_x and ω_y,

$$\ddot{x} = 0.2(1-x^2)\dot{x} - \omega_x^2 x + \xi_x + 0.03(y-x),$$

$$\ddot{y} = 0.2(1-y^2)\dot{y} - \omega_y^2 y + \xi_y + \mu(x-y), \tag{12}$$

where $\omega_x=1.02$, $\omega_y=0.98$, and ξ_x and ξ_y are independent Gaussian white noise with standard deviation 0.04. This example has been considered in [8,12]. The equations have been integrated with the Euler scheme and the sampling time was 0.1π. The variables x and y have been used to reconstruct the phase space with embedding dimension 10 and delay 12, as in the former case. The thresholds ε_X and ε_Y have been chosen such that for symmetrical coupling $\langle p(\vec{x}_i)\rangle=\langle p(\vec{y}_i)\rangle=0.1$. The results for the indices MCR are shown in Figs. 3(c) and 3(d) in dependence on the coupling strength μ. For $\mu<0.03$, $M_{CR}(X|Y)<M_{CR}(Y|X)$, since the coupling is stronger from Y to X than vice versa. At the coupling strength 0.03, we obtain $M_{CR}(X|Y)=M_{CR}(Y|X)$, be-

cause the coupling is symmetrical, and for $\mu > 0.03$, we observe that $M_{CR}(X|Y) > M_{CR}(Y|X)$, because the coupling from X to Y is stronger than vice versa. Note that at $\mu \approx 0.06$ both oscillators become phase synchronized and the value of $M_{CR}(Y|X)$ increases much faster.

C. Structurally different systems

Next, we study the more challenging case of two structurally different systems, namely a stochastic Van der Pol system which drives a Rössler system. The equation of the driving system X is

$$\ddot{x} = 0.1(1 - x^2)\dot{x} - \omega_x^2 x + \xi_x, \tag{13}$$

where $\omega_x = 0.98$ and ξ_x is Gaussian white noise with standard deviation 0.05. The equations of the response system Y are given by

$$\dot{y}_1 = -y_2 - y_3,$$

$$\dot{y}_2 = y_1 + 0.15y_2 + \mu x,$$

$$\dot{y}_3 = (y_1 - 10)y_3 + 0.2. \tag{14}$$

The equations have been integrated with a Euler scheme and the sampling time was 0.1π. The phase space has been reconstructed using the variables x and y_1 and embedding dimension 10 and delay 12. The values of the thresholds ε_X and ε_Y have been chosen as in the former cases. The curves for MCR are shown in dependence on the coupling strength μ in Fig. 4. In this interval of values of the coupling strength both systems are before the onset of phase synchronization [12]. For all values of the coupling strength we obtain $M_{CR}(X|Y) > M_{CR}(Y|X)$, i.e., we are able to detect the direction of the coupling also in this case.

IV. CHOICE OF THE PARAMETERS

In order to compute the indices MCR, we need to fix four parameters: the embedding dimension m and the delay τ for the reconstruction of the phase space, and the thresholds ε_X and ε_Y for the computation of the recurrence matrices. As we have mentioned in the previous section, the special choice of the embedding parameters does not influence the results. In Fig. 5 we show the results for the direction parameters MCR for different choices of m and τ for the two identical unidirectionally coupled Hénon systems [Eqs. (8) and (9)]. We obtain, regardless of the choice of the embedding parameters, $M_{CR}(X|Y) > M_{CR}(Y|X)$ for all values of the coupling strength μ before the onset of synchronization. This is the correct behavior, since the system X is the driver and Y is the response.

With regard to the choice of the thresholds ε_X and ε_Y, we have mentioned in the previous section that they were chosen such that the mean probabilities of recurrence for both systems at coupling strength $\mu = 0$ are equal. In this way, it is not necessary to normalize the data x_i and y_i beforehand. In the numerical examples considered in Sec. III, we chose the mean probability of recurrence to be equal to 0.01. In order to demonstrate how the results depend on this choice, we show in Fig. 6 $\Delta M_{CR} = M_{CR}(X|Y) - M_{CR}(Y|X)$ in dependence on the coupling strength and on the mean probability of recurrence (labeled as "recurrence rate" in the plot) for the

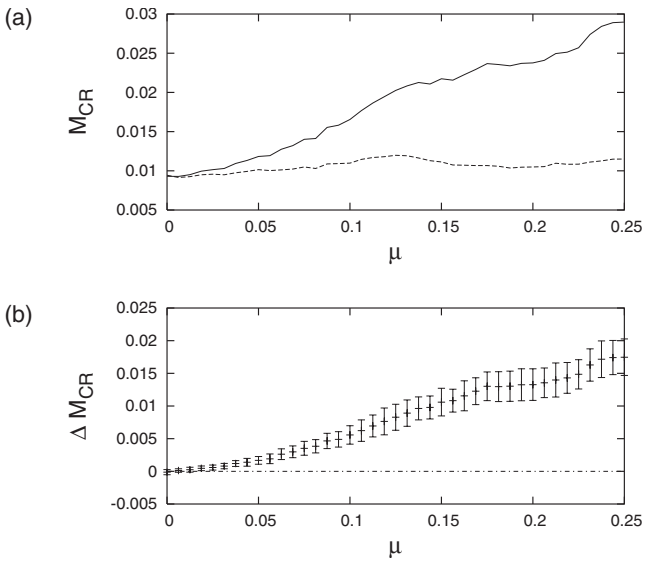

FIG. 4. (a) Mean conditional probabilities of recurrence $M_{CR}(X|Y)$ (solid) and $M_{CR}(Y|X)$ (dashed) for the chaotic Rössler system driven by the stochastic Van der Pol system. For each value of the coupling strength μ, the mean value over 100 trajectories for uniformly distributed initial conditions has been computed. The system X is the driver, and hence, we find $M_{CR}(X|Y) > M_{CR}(Y|X)$. (b) Mean value of the difference $\Delta M_{CR} = M_{CR}(X|Y) - M_{CR}(Y|X)$ and corresponding standard deviation over 100 trajectories. The zero line is also plotted for orientation (dotted-dashed line).

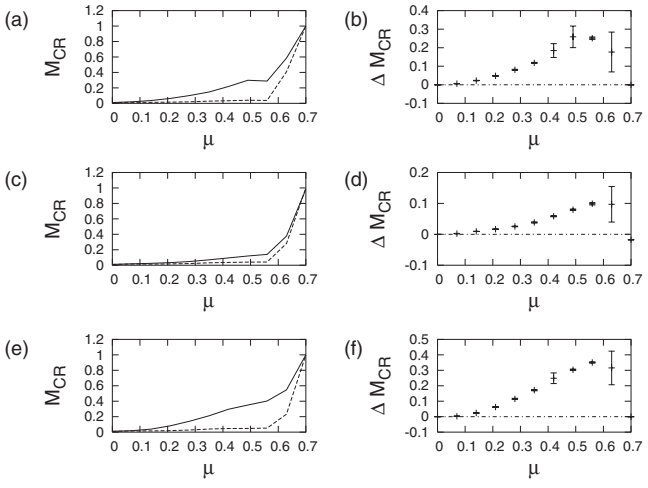

FIG. 5. Mean conditional probabilities of recurrence $M_{CR}(X|Y)$ (solid) and $M_{CR}(Y|X)$ (dashed) for two identical unidirectionally coupled Hénon maps for different choices of the embedding parameters: (a) $m=3$, $\tau=1$, (c) $m=2$, $\tau=3$, (e) $m=5$, $\tau=1$. For each value of the coupling strength μ, the mean value over 10 trajectories for uniformly distributed initial conditions has been computed. In (b), (d), and (f) the mean value and standard deviation over 10 trajectories of the corresponding ΔM_{CR} are represented. The zero line is also plotted for orientation (dotted-dashed line).

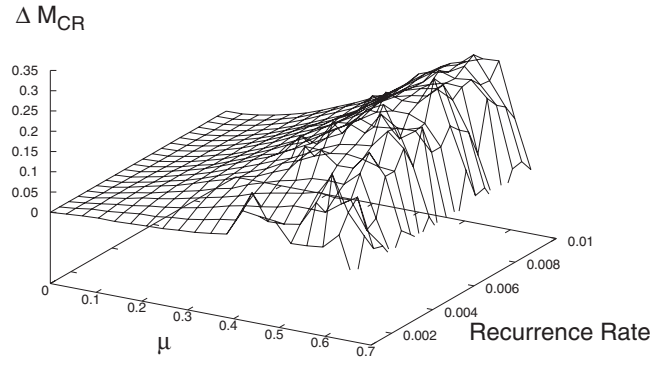

FIG. 6. $\Delta M_{CR}=M_{CR}(X|Y)-M_{CR}(Y|X)$ for two identical unidirectionally coupled Hénon maps in dependence on the coupling strength μ and the mean probability of recurrence or recurrence rate. For each value of the coupling strength μ, the mean value over 10 trajectories for uniformly distributed initial conditions has been computed.

Hénon systems, Eqs. (8) and (9). As system X is the driver, we expect that the surface ΔM_{CR} takes only positive values, which is the case in fact. Hence, we see that the estimation of MCR does not depend crucially on the choice of the thresholds ε_X and ε_Y. Hence, for a rather broad range of values of the thresholds, the direction of the coupling can be estimated correctly.

V. INFLUENCE OF NOISE

We now study the influence of observational noise on the MCR measures [Eqs. (5) and (6)]. Therefore, we add different levels of noise to the scalar time series $\{x_i\}_{i=1}^N$ and $\{y_i\}_{i=1}^N$, so that we compute the MCR indices for the series $x_i'=x_i+\gamma\sigma_x\eta_i^x$ and $y_i'=y_i+\gamma\sigma_y\eta_i^y$, where γ denotes the level of noise, σ_x and σ_y are the standard deviation of x_i and y_i, respectively, and η_x and η_y are two independent realizations of uniformly distributed random noise between -0.5 and 0.5. Figure 7 shows the results obtained for the MCR indices for three different values of γ corresponding to 20%, 40%, and 60% of observational noise.

We observe that when the level of noise γ increases, it becomes more difficult to detect the asymmetry of the coupling for very small values of the coupling strength μ, because both curves $M_{CR}(X|Y)$ and $M_{CR}(Y|X)$ are almost equal. The larger the level of noise, the stronger must be the coupling strength in order to detect the asymmetry. Nevertheless, even with such high levels of observational noise, the asymmetry of the coupling can still be correctly detected for relatively small values of the coupling strength. Hence, we conclude that the MCR indices are a rather robust measure for the detection of the asymmetry of the coupling, also in the presence of high levels of observational noise.

VI. PASSIVE EXPERIMENTS

One crucial problem of all measures for the detection of asymmetry of the coupling is the assessment of the significance of the results for passive experiments, i.e., when the coupling strength between both systems X and Y cannot be

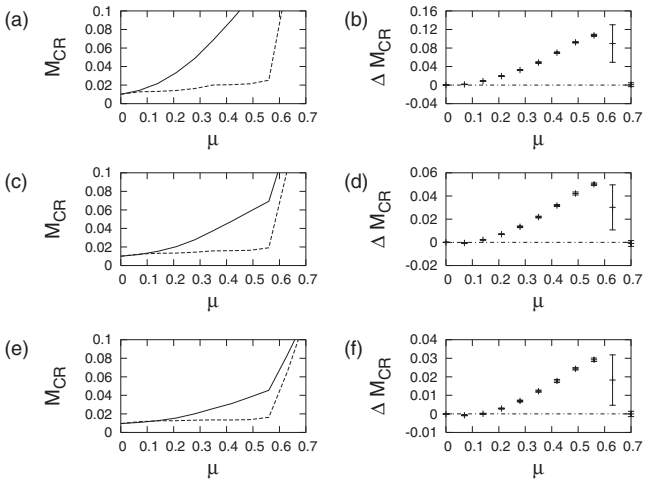

FIG. 7. $M_{CR}(X|Y)$ and $M_{CR}(Y|X)$ for two identical unidirectionally coupled Hénon maps contaminated by uniformly distributed noise in dependence on the coupling strength μ. (a) $\gamma=0.2$, (c) $\gamma=0.4$, (e) $\gamma=0.6$. For each value of the coupling strength μ, the mean value over 10 trajectories for uniformly distributed initial conditions has been computed. In (b), (d), and (f) the corresponding mean value of the difference ΔM_{CR} and the standard deviation over 10 trajectories are plotted. The zero line is also plotted for orientation (dotted-dashed line).

varied systematically in experiments. In such cases, we usually just have one scalar measurement sequence for each system $\{x_i\}_{i=1}^N$ and $\{y_i\}_{i=1}^N$ for a fixed coupling strength μ. This is the case in numerous situations. For example, the experimental data used in [6] to illustrate the applicability of the method for the detection of the asymmetry of the coupling, are time series of breath rate and instantaneous heart rate of a sleeping human. It is very hard, if not impossible, to change the coupling strength between the respiratory and cardiological system of a person in a systematic way. The authors in [4] apply their proposed method for the detection of asymmetry of the coupling to intracranially recorded electroencephalogram (EEG) data. In this case, it is also obvious that it is not possible to change the coupling strength between different areas of the brain, in a controlled manner.

In all these cases we obtain just one value for the directionality indices and then it is not trivial to decide whether the computed values have been obtained just by chance or whether they are significant. In order to address this question, we propose the following statistical test. Our null hypothesis is that the two systems X and Y are independent. To test this null hypothesis, we generate the so-called *natural or twin surrogates* [27]. Suppose that we have one time series for each system $\{x_i\}_{i=1}^N$ and $\{y_i\}_{i=1}^N$ for a fixed coupling strength μ. The natural surrogates are trajectories from the same underlying dynamical systems X and Y with identical coupling strength μ between both of them, but starting at different initial conditions. We denote them by $\{x_i^s\}_{i=1}^N$ and $\{y_i^s\}_{i=1}^N$. If we have computed the directionality indices $M_{CR}(x|y)$ and $M_{CR}(y|x)$ for the measured time series, we can compare the obtained values with the distribution of $M_{CR}(x|y^s)$ and $M_{CR}(y^s|x)$ [29], respectively, generated from a large number of surrogates. If both systems X and Y are

independent, the value $M_{CR}(x|y)$ will not differ significantly from the distribution of the values $M_{CR}(x|y^s)$. Otherwise, we can reject the null hypothesis, indicating that the obtained values for the directionality indices are significant.

At this point, the following question arises naturally: dealing with experimental data, one usually does not have a model for the governing dynamics. Then, how can one generate natural surrogates? The answer to this question has been addressed in [27], where an algorithm based on recurrence has been proposed to generate natural surrogates without knowing the underlying equations of the system. These recurrence based surrogates are called *twin surrogates* and have been applied in [27] to tackle the problem of passive experiments in phase synchronization.

We now show the performance of the MCR method applying the twin surrogates test to analyze the estimation of the asymmetry of the coupling in Eqs. (8) and (9). We therefore generate 100 twin surrogates using the algorithm presented in [27]. We assume that we have scalar time series, and hence, use delay embedding to reconstruct the trajectory. We use embedding dimension $m=3$ and delay $\tau=1$, as in Sec. III. The threshold for the generation of the surrogates is chosen to be $\delta=0.09$ (see [27] for further details), according to the procedure given in [28]. Summarizing, the following steps have to be undertaken for each value of the coupling strength μ:

(i) Choose the significance level α.

(ii) Compute $M_{CR}(x|y)$ and $M_{CR}(y|x)$.

(iii) Generate L twin surrogate time series $\{x_i^{s_j}\}_{i=1}^N$ and $\{y_i^{s_j}\}_{i=1}^N$, with $j=1,\ldots,L$.

(iv) Compute $M_{CR}(x|y^{s_j})$ and $M_{CR}(y^{s_j}|x)$ for $j=1,\ldots,L$.

(v) Compute the α-significance value based on the distribution obtained in the former step.

(vi) If $M_{CR}(x|y)$ and $M_{CR}(y|x)$ are larger than the corresponding α-significance values, reject the null hypothesis.

The results for Eqs. (8) and (9) are shown in Fig. 8.

The values of $M_{CR}(X|Y)$ and $M_{CR}(Y|X)$ are above the significance level in both cases for all values of the coupling strength. Hence, the null hypothesis is correctly rejected. Therefore, in the case that we have a passive experiment, this procedure can be applied to assess the significance of the results about the asymmetry of the coupling.

Note that in the case of passive experiments, we cannot apply the criterion proposed in Sec. II to choose the thresholds ε_X and ε_Y, such that for coupling strength equal to zero we have $\langle p(\vec{x}_i)\rangle=\langle p(\vec{y}_i)\rangle$, because we do not know the value of the coupling strength. Therefore, one has to apply another criterion to choose the thresholds ε_X and ε_Y. In the example shown in Fig. 8 we have normalized the data beforehand to have zero mean and standard deviation equal to one, and then we have chosen $\varepsilon_X=\varepsilon_Y=0.1$. If both interacting systems are structurally similar, then $M_{CR}(X|Y)$ will be approximately equal to $M_{CR}(Y|X)$ for coupling strength equal to zero. However, if the interacting systems are structurally different, this approach might not hold anymore.

VII. COMPARISON WITH OTHER METHODS

As mentioned in the introduction, several methods have been proposed in the literature to estimate the direction of the coupling. Most of these methods can be divided into the following three categories: (i) methods based on a functional relationship between the phases [8], (ii) state-space based methods [3–5], and (iii) information theory based methods [6,7].

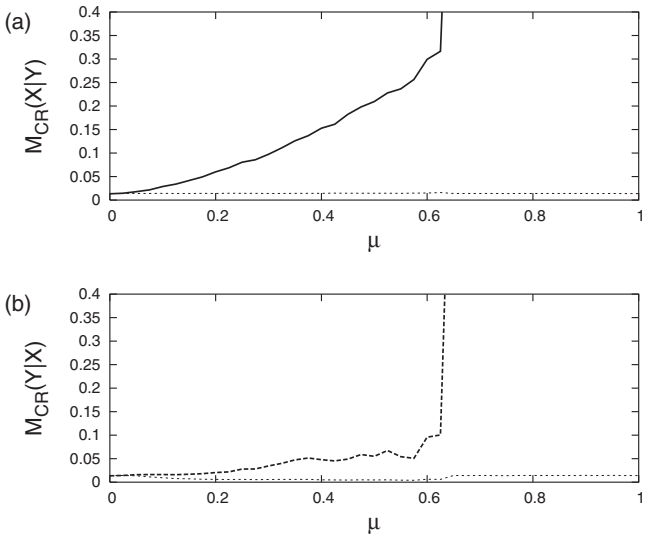

FIG. 8. (a) Mean conditional probability of recurrence $M_{CR}(X|Y)$ (solid) and 1% significance level (dotted) for two identical Hénon maps unidirectionally coupled. (b) $M_{CR}(Y|X)$ (dashed) and 1% significance level (dotted) for the same system. 100 twin surrogates have been generated to estimate the significance level. The data have been normalized beforehand to have zero mean and standard deviation equal to one and $\varepsilon_X=\varepsilon_Y=0.1$.

(i) In order to apply the method introduced in [8], one has to estimate first the phases of the interacting systems and then fit a functional relationship between them. From this function, the directionality parameters are then derived. The main disadvantage of this method is that it is not always possible to assign a phase to a system based on a scalar time series, especially if the power spectrum of the signal does not present a predominant peak (i.e., one cannot speak of a main frequency of rotation of the system).

(ii) The state-space methods are based on the relationship between neighbors in the respective phase spaces of the interacting systems X and Y. At a first glance, these methods might seem to be very close to the recurrence based method introduced in this paper. However, there are some important differences between them. For example, the computed indices in [4,5] are based on the mean distances between a certain number q of nearest neighbors, i.e., they use the matrix of distances $|\vec{x}_i-\vec{x}_j|$ between all points of the trajectory. In contrast, the MCR indices do not use the distance matrix explicitly but rather the matrix of inequalities $|\vec{x}_i-\vec{x}_j|<\varepsilon$. Another way to express this difference is the following: in the state-space based methods, the threshold used to compute the neighbors is different for each point of the trajectory $\vec{x}_i$, i.e., $\varepsilon=\varepsilon(i)$, whereas to compute MCR the threshold is the same for all points of the trajectory. Another important difference is that in the MCR method, once the threshold is fixed, it remains the same for all different values of the coupling strength. In contrast, in the state-space based methods,

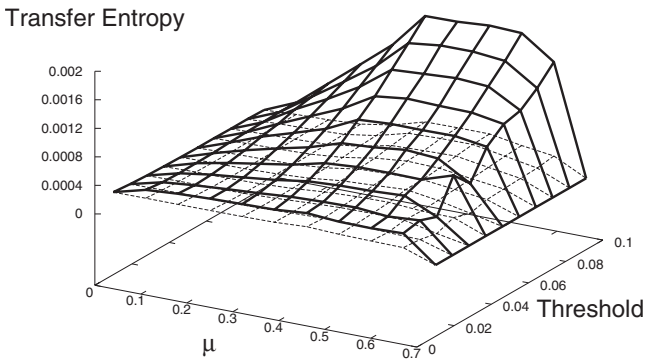

FIG. 9. Transfer entropy for two identical unidirectionally coupled Hénon maps in dependence on the coupling strength μ and the threshold. For each value of the coupling strength μ, the mean value over 10 trajectories for uniformly distributed initial conditions has been computed. Solid surface: transfer entropy from X to Y; dashed surface: transfer entropy from Y to X.

the threshold does not only depend on the point of the trajectory, but also on the coupling strength.

(iii) Actually, the MCR method is closer to the information theory based methods, e.g., the transfer entropy [6]. In both cases, conditional probabilities of recurrence are estimated. But in the case of the transfer entropy, transition probabilities are considered, rather than static ones. This has the advantage of incorporating dynamical structure. The disadvantage compared to the MCR indices is that the number of data points needed for the estimation is considerable, and this might hamper the application of this method to experimental time series. For example, using the same number of data points (10 000) and the same range of values of the threshold as with the MCR method (Fig. 6) for the analysis of the direction of the coupling of Eqs. (8) and (9), we obtain the results for the transfer entropy as given in Fig. 9. The transfer entropy from X to Y is represented by the solid surface and the transfer entropy from Y to X by the dashed one. Note that even though the coupling is purely unidirectional, the transfer entropy from Y to X is larger than zero (it becomes only zero for coupling strength $\mu \geqslant 0.7$, when synchronization sets in). That means that the transfer entropy does not detect that the coupling is purely unidirectional. This problem might be overcome using longer data sets. In the case of the MCR method, a purely undirectional coupling can be easily detected by computing the recurrence rate of the driver in dependence on the coupling strength, which will then be constant.

VIII. CONCLUSIONS

In this paper, we have proposed indices for the detection of the asymmetry of the coupling between interacting systems. The quantification of the asymmetry of the coupling can be very helpful in identifying driver-response relationships, which is a relevant problem in many fields, especially when dealing with experimental time series. The proposed indices are based on the mean conditional probabilities of recurrence (MCR). We have exemplified their applicability by several numerical examples which are representative of strong and weak coupled systems. Furthermore, we have shown that the MCR indices can also cope with the more challenging case of structurally different systems. We have studied the dependence of the MCR indices on the parameters needed for their estimation and we have found out that the choice of the parameters is not crucial for the correct detection of the asymmetry of the coupling. Moreover, we have addressed the very relevant problem of the quantification of the direction of the coupling in passive experiments and proposed an algorithm to assess the statistical significance of the results. Furthermore, we have studied the influence of observational noise on our method and compared it with other existing techniques for the detection of the asymmetry of the coupling. The numerical examples we considered in this paper were mainly low dimensional. The application of this technique to high-dimensional systems, as well as to experimental time series will be addressed in a forthcoming paper.

ACKNOWLEDGMENTS

This work has been supported by the DFG priority program 1114 (Contract No. DFG-KL 955), the network of excellence BIOSIM (Contract No. LSHB-CT-2004-005137) and the RCUK.

[1] A. S. Pikovsky, M. G. Rosenblum, and J. Kurths, *Synchronization: A Universal Concept in Nonlinear Sciences*, Cambridge Nonlinear Science Series 12 (Cambridge University Press, Cambridge, 2001).
[2] S. Boccaletti, J. Kurths, G. Osipov, D. L. Valladares, and C. S. Zhou, Phys. Rep. **366**, 1 (2002).
[3] S. J. Schiff, P. So, T. Chang, R. E. Burke, and T. Sauer, Phys. Rev. E **54**, 6708 (1996).
[4] J. Arnhold, K. Lehnertz, P. Grassberger, and C. E. Elger, Physica D **134**, 419 (1999).
[5] R. QuianQuiroga, J. Arnhold, and P. Grassberger, Phys. Rev. E **61**, 5142 (2000).
[6] T. Schreiber, Phys. Rev. Lett. **85**, 461 (2000).
[7] M. Palus, V. Komarek, Z. Hrncir, and K. Sterbova, Phys. Rev. E **63**, 046211 (2001).
[8] M. G. Rosenblum and A. S. Pikovsky, Phys. Rev. E **64**, 045202(R) (2001).
[9] H. Kantz and T. Schreiber, *Nonlinear Time Series Analysis* (Cambridge University Press, Cambridge, 1997).
[10] N. F. Rulkov, M. M. Sushchik, L. S. Tsimring, and H. D. I. Abarbanel, Phys. Rev. E **51**, 980 (1995).
[11] L. Kocarev and U. Parlitz, Phys. Rev. Lett. **76**, 1816 (1996).
[12] D. A. Smirnov and R. G. Andrzejak, Phys. Rev. E **71**, 036207 (2005).

[13] M. Palus and A. Stefanovska, Phys. Rev. E **67**, 055201(R) (2003).
[14] C. Stam and B. van Dijk, Physica D **163**, 236 (2002).
[15] M. C. Romano, M. Thiel, J. Kurths, I. Z. Kiss, and J. Hudson, Europhys. Lett. **71**, 466 (2005).
[16] H. Poincaré, Acta Math. **13**, 1 (1890).
[17] V. Afraimovich, Chaos **7**, 12 (1997).
[18] B. Saussol and J. Wu, Nonlinearity **16**, 1991 (2003).
[19] R. Gilmore and M. Lefranc, *The Topology of Chaos: Alice in Stretch and Squeezeland* (Wiley, New York, 2002).
[20] J.-P. Eckmann, S. O. Kamphorst, and D. Ruelle, Europhys. Lett. **5**, 973 (1987).
[21] N. Marwan, N. Wessel, U. Meyerfeldt, A. Schirdewan, and J. Kurths, Phys. Rev. E **66**, 026702 (2002).
[22] N. Marwan, M. C. Romano, M. Thiel, and J. Kurths, Phys. Rep. **438**, 237 (2007).
[23] M. Thiel, M. C. Romano, P. L. Read, and J. Kurths, Chaos **14**, 234 (2004).
[24] M. Thiel, M. C. Romano, and J. Kurths, Phys. Lett. A **330**, 343 (2004).
[25] M. C. Romano, M. Thiel, J. Kurths, and W. von Bloh, Phys. Lett. A **330**, 214 (2004).
[26] C. Stam, B. F. Jones, G. Nolte, M. Breakspear, and P. Scheltens, Cereb. Cortex **17**, 92 (2007).
[27] M. Thiel, M. C. Romano, J. Kurths, M. Rolfs, and R. Kliegl, Europhys. Lett. **75**, 535 (2006).
[28] M. Romano, M. Thiel, J. Kurths, K. Mergenthaler, and R. Engbert (unpublished).
[29] Note that considering $M_{CR}(x^s|y)$ and $M_{CR}(y|x^s)$ would yield the same result.